行政院國家科學委員會專題研究計畫成果報告

鮭魚產卵礫石河床形貌引發之壓力差試驗探討

Bedform-Induced Pressure Drop across Spawning Gravels

計畫編號：NSC 89-2211-E-002-142

執行期限：89 年 8 月 1 日至 90 年 7 月 31 日

主持人：吳富春　　國立台灣大學生物環境系統工程學系

中文摘要

本研究針對鮭魚產卵之礫石河床形貌所引發之壓力差及孔隙流速進行水理試驗，探討鮭魚產卵礫石河床形貌壓差與水流流況、河床形貌因子、河道坡度、礫石粒徑間之定量關係，利用此一關係可精確估計孔隙水流速度，進而評估礫石河床中鮭魚卵之存活率，做為後續規劃棲地復育方案之有效工具。

關鍵詞：鮭鱒魚、產卵礫石河床、河床形貌、壓力差、孔隙水流速度。

Abstract

The purposes of this experimental study is to investigate the bedform-induced pressure drop across spawning gravels and develop a quantitative relationship between the pressure drop and the flow condition, geomorphologic factor, streambed slope, and grain sizes of spawning gravels. Such a relationship can be used to make an accurate estimation of the apparent velocity and further assess the egg survival rate. The proposed quantitative model may well serve as an effective tool for planning of habitat restoration project.

Keywords: Salmonids, spawning gravels, bedform, pressure drop, apparent velocity.

1. Introduction

Natural gravel-bed streams provide suitable locations for salmonids (salmon and trout) to construct their spawning nests (or redds). The typical spawning redd (shown in Fig. 1) consists of an upstream pit and a downstream tailspill under which the fertilized eggs are protected against the bedload motion and scour during the high flows (Burner 1951; Chapman 1988).

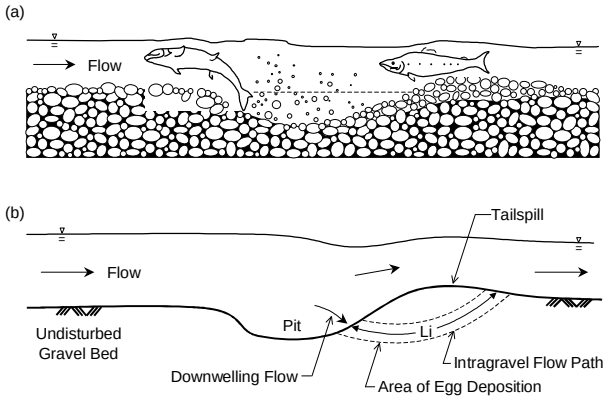

Fig. 1. (a) Diagram of redd making; (b) Typical morphology of spawning redd and sketch of intragravel flow

Thibodeaux and Boyle (1987) pointed out that the general pattern of the surface flow across this type of bedform is analogous to the flow condition around circular cylinders. A pressure drop must exist between the upstream face of the bedform and the vortex region on the downstream face. Field and laboratory observations have indicated that the hydrodynamics induced by the bedform promotes a downwelling flow into the spawning gravels, as illustrated in Figure 1. Such a flow is beneficial for the exchange of dissolved oxygen and removal of metabolic waste, thus maintains the aquatic environment required for incubation success. For example, Cooper's data showed that the survival rates corresponding to the apparent velocities of 0.034 cm/s and 0.0004 cm/s are 89% and 2%, respectively. Therefore, the apparent velocity may well

serve as an indicator for embryo-survival assessment (Wu 2000). To evaluate the apparent velocity (V') of the intragravel flow, a number of investigators have employed Darcy's equation, which can be expressed by:

$$V' = K \cdot (\Delta h / L_i) \qquad (1)$$

where $K =$ hydraulic conductivity of the spawning gravels; $\Delta h =$ pressure-head drop between the upstream and downstream faces of tailspill; $L_i =$ length of the intragravel flow path (Fig. 1).

The pressure drop across the sand-coated two-dimensional triangular elements has been measured and reported as a local pressurecoefficient (Vittal et al. 1977). Their test results showed that the distribution of pressure drop varies primarily with the geometry of the triangular element (such as shape factor and relative form roughness). The shape factor is the ratio between the height and length of the roughness element; the relative form roughness is the ratio of element height to flow depth. To accurately evaluate the pressure drop across the redd gravels, a series of physical model tests using pervious bed materials should be conducted. This experimental study aims to investigate the pressure drop across the form roughness in the porous streambed. Such a study provides more practical information for estimation of the intragravel flow velocity and, therefore, assessment of the salmonid embryo survival.

2. Dimensional Analysis

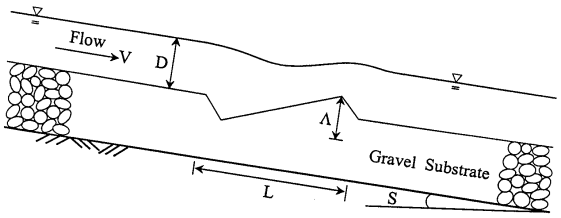

Fig. 2. Definition sketch of experimental setup

The total pressure-head drop across a form roughness is varying as a function of bedform geometry and surface flow hydraulics. For the pervious bedform roughness, the permeability of the porous medium affects the flow in the boundary layer and thus the pressure drop between the upstream and downstream faces of the form roughness. In addition, the slope of the streambed, gravity, and fluid viscosity also play significant roles in the system. The relationship between the pressure-head drop and these physical quantities may be expressed as:

$$\Delta h = f(V, D, \Lambda, {}^{a}, d_g, S, \neg, g) \qquad (2)$$

in which $V =$ average approaching velocity of the surface flow (definition sketch shown in Figure 2); $D =$ depth of the approaching surface flow; $\Lambda =$ height of the spawning redd; ${}^{a} = \Lambda / L_r =$ shape factor of the spawning redd, where $L_r =$ length of the spawning redd; $d_g =$ grain size of the bed material; $S =$ mean slope of the streambed; $\neg =$ kinematic viscosity of water; $g =$ gravitational acceleration. The dimensional analysis gives:

$$\frac{\Delta h}{(V^2/2g)} = f\left(\mathrm{Fr}, \frac{\Lambda}{D}, {}^{a}, \mathrm{Re}, S\right) \qquad (3)$$

in which $\mathrm{Fr} = V/\sqrt{gD} =$ Froude number of the approaching flow; Λ / D represents the relative form roughness; $\mathrm{Re} = V \cdot d_g / \neg =$ grain Reynolds number.

3. Ranges of Experimental Variables

Since the present study is focused on the pressure drop across the spawning redd in natural gravel-bed rivers, the similitude laws between the prototype and the model must be followed, which include geometric similarity (^{a}, Ë/D, S) , kinematic similarity [$\Delta h/(V^2/2g)$], and dynamic similarity (Fr , Re). The possible ranges of the testing variables are summarized in Table 1.

Table 1. Ranges and fractions of experimental variables

Variable	Range	Fraction	Sources of data
Froude number, Fr	0-0.1	4/90	
	0.1-0.2	20/90	Kondolf et al. (1993)
	0.2-0.3	43/90	
	0.3-0.4	18/90	
	0.4-0.5	4/90	
	0.5-0.6	1/90	
Shape factor, a	1/20 - 1/5		Burner (1951) Kondolf et al. (1993)
Relative form roughness, Λ / D	0-0.3	12/60	Burner (1951)
	0.3-0.6	22/60	
	0.6-0.9	10/60	Kondolf et al. (1993)
	0.9-1.2	8/60	
	1.2-1.5	2/60	
	1.5-2.0	6/60	
Bed slope, S	0 - 1/1000	1/36	Kondolf et al. (1993)
	1/1000 - 3/1000	21/36	
	3/1000 - 5/1000	10/36	
	5/1000 - 10/1000	2/36	
	10/1000 - 30/1000	2/36	
Grain Reynolds number, Re	2,000-4,000	3/38	Kondolf et al. (1993)
	4,000-6,000	4/38	
	6,000-8,000	6/38	
	8,000-10,000	6/38	
	10,000-12,000	4/38	
	12,000-14,000	5/38	
	14,000-16,000	3/38	
	16,000-18,000	1/38	
	18,000-20,000	2/38	
	20,000-22,000	1/38	
	22,000-25,000	3/38	

4. Experiments

The experiments are conducted in a 0.4-m wide by 12-m long circulating and slope-adjustable flume. Three series of tests (Series C, M, and F) are performed with coarse, medium, and fine gravels. The median grain sizes for these gravels are 21.9 mm, 13.3 mm, and 6.5 mm, respectively. Measurements of the pressure heads are made with the Fiber Optics Probes (FOP) when the flow achieves a steady condition. A total of 70 sets of data are obtained in this study.

5. Results

(1) Classification of Surface Profile

Three types of surface profile can occur above the bedform, depending on the relative form roughness and the grain Reynolds number (shown in Figure 3). The criterion for classifying drop and non-drop type profiles is $(\Lambda / D)^{0.75}(\mathrm{Re})^{0.25} = 4.3$. For $(\Lambda / D)^{0.75}(\mathrm{Re})^{0.25} > 4.3$, the surface profile belongs to drop type, whereas for $(\Lambda / D)^{0.75}(\mathrm{Re})^{0.25} < 4.3$, the water surface is non-drop type profile. For those data between $(\Lambda / D)^{0.75}(\mathrm{Re})^{0.25} = 4.3 \pm 10\%$, their profiles belong to transition type.

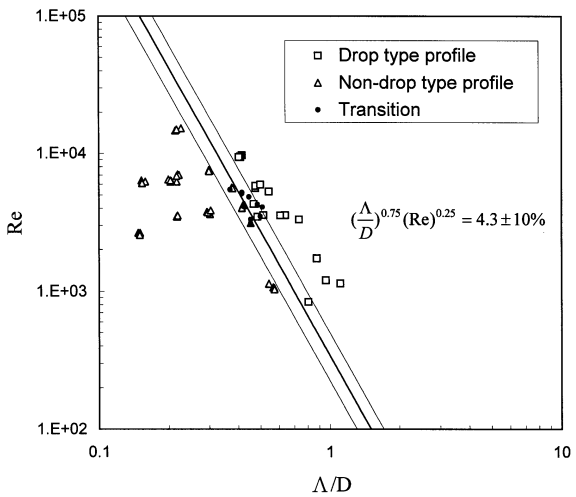

Fig. 3. Classification of surface profile

(2) Dimensionless Pressure Drop

The dimensionless form of the pressure drop as a function of flow and bedform parameters can be expressed as: $\Delta h/(V^2/2g) = 10^a \mathrm{Fr}^b (\Lambda / D)^{c\ a d} \mathrm{Re}^e S^f$. For drop type profile: $a = 3.55$, $b = 3.72$, $c = 1.80$, $d = -0.39$, $e = -0.29$, $f = 1.71$, with $R^2 = 0.89$. For non-drop type profile: $a = 2.31$, $b = -2.26$, $c = 0.97$, $d = -0.24$, $e = -0.27$, $f = 1.01$, with $R^2 = 0.79$. The comparison of the experimental and calculated dimensionless pressure drop is shown in Figure 4.

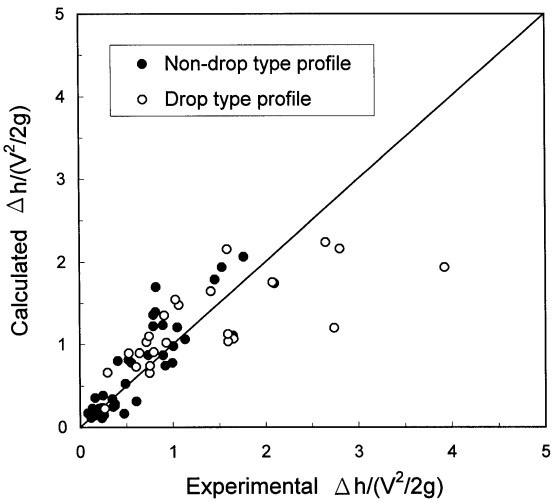

Fig. 4. Comparison of experimental and calculated press drop

(3) Darcy (Apparent) Velocity

The relationships between hydraulic gradient and Darcy velocity are shown in Figure 5 for different gravel sizes. The theoretical curves are based on the relations proposed by Legrand (2001) and Trussell and Chang (1999). The graph reveals an excellent agreement between the experimental and theoretical results.

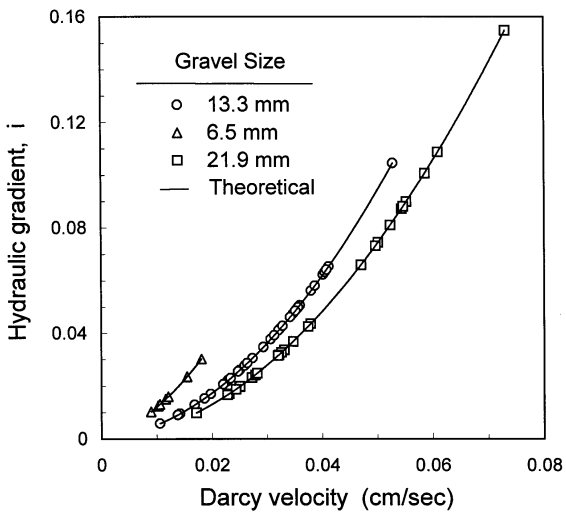

Fig. 5. Relationship between hydraulic gradient and Darcy velocity

(4) Hydraulic Gradient

A non-linear regression analysis leads to the following result, with $R^2 = 0.69$:

$$i = \exp(C_1 + C_2 X + C_3 X^2 + C_4 X^3)$$

$$X = \mathrm{Fr}^{C_5} (\Lambda / D)^{C_6} a^{C_7} \mathrm{Re}^{C_8} S^{C_9}$$

where $C_1 = 3.23\times10^5$, $C_2 = -7.06\times10^5$, $C_3 = 4.41\times10^5$, $C_4 = -5.85\times10^5$, $C_5 = -2.99\times10^{-4}$, $C_6 = 3.51\times10^{-4}$, $C_7 = -1.89\times10^{-4}$, $C_8 = 4.68\times10^{-5}$, $C_9 = 5.64\times10^{-4}$. The relationship is shown in Figure 6. Once the hydraulic gradient is determined with the above equation, it can be used to evaluate the apparent velocity for planning and design of the restoration and improvement of salmonid spawning habitats.

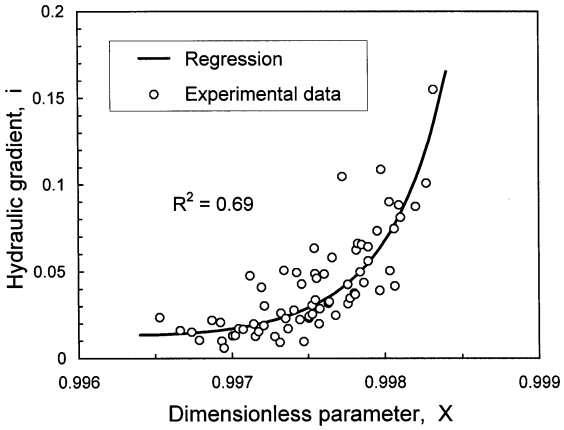

Fig. 6. Relationship between hydraulic gradient and parameter X

References

1. Kondolf, G. M., M. J. Sale, and M. G. Wolman, Modification of fluvial gravel size by spawning salmonids, Water Resour. Res., 29, 2265-2274, 1993.
2. Thibodeaux, L. J., and J. D. Boyle, Bedform-generated convective transport in bottom sediment, Nature, 325, 341-343, 1987.
3. Vittal, N., K. G. Ranga Raju, and R. J. Garde, Resistance of two dimensional triangular roughness, J. Hydraul. Res. IAHR, 15, 19-36, 1977.
4. Wu, F.-C., Modeling embryo survival affected by sediment deposition into salmonid spawning gravels: Application to flushing flow prescriptions, Water Resour. Res., 36, 1595-1603, 2000.